RAPID COMMUNICATIONS

PHYSICAL REVIEW A VOLUME 38, NUMBER 1 JULY 1, 1988

Structure of a fluid interface near the critical point

James W. Schmidt
Thermophysics Division, National Bureau of Standards, Gaithersburg, Maryland 20899

(Received 16 March 1988)

The structure of the liquid-liquid interface of three very different mixtures (carbon disulfide + methanol, methanol + cyclohexane + deuterated cyclohexane, and nitrobenzene + n-decane) has been studied using ellipsometry in the reduced temperature range $0.0009 < t < 0.042$. Although the elliptical thickness varies by an order of magnitude between these mixtures, the data from all three mixtures can be scaled to the same universal constant by a combined mean-field plus capillary-wave model of the interface. The universal constant determined experimentally is significantly less than the theoretical value.

When two fluid phases coexist, the order parameter changes smoothly as one crosses the interface between the two phases. Mean-field theories of the interface[1–3] predict an order-parameter profile with a transition region whose thickness is only a function of the bulk correlation length ξ^-. When capillary waves are added to the theory,[4–6] the thickness of the interface increases and becomes a function of a long-wavelength cutoff (which is usually determined by an external field or the area of the interface) and a short-wavelength cutoff l^*. The short-wavelength cutoff is the length that sets the smallest scale on which capillary waves can be defined.

We have used ellipticity measurements (see Fig. 1) of the liquid-liquid interface in the binary fluid carbon disulfide (CS_2) + methanol (CH_3OH) from room temperature to within 0.2 K of the consolute point at $T_c = 309$ K and we have compared these data with the Fisk-Widom[3] version of mean-field theory. The data from this mixture and two other mixtures, methanol (CH_3OH) + cyclohexane (C_6H_{12}) + deuterated cyclohexane (C_6D_{12}), and nitrobenzene ($C_6H_5NO_2$) + n-decane ($C_{10}H_{22}$) are consistently 20% to 30% higher than the mean-field values. Adding capillary waves to mean-field theory moves the theoretical curve in the right direction but overcorrects by a significant amount for all three mixtures.

The ellipticity ρ is the imaginary part of the reflectivity ratio and is a measure of the optical thickness of the interface. $\bar{\rho}$ can be calculated at Brewster's angle θ_B from an equation derived by Drude:[7]

$$\bar{\rho}_D = \mathrm{Im}\frac{r_p}{r_s} = \frac{\pi}{\lambda}[(n_-^2 + n_+^2)^{1/2}/(n_-^2 - n_+^2)]\eta \,, \tag{1a}$$

with

$$\eta = \int \frac{[n^2(z) - n_-^2][n^2(z) - n_+^2]}{n^2(z)} dz \,. \tag{1b}$$

Here $n(z)$ is the refractive index profile perpendicular to the interface and n_- and n_+ are the refractive indices deep in the interiors of the respective bulk phases. n_- and n_+ (the refractive indices for the upper and lower phases, respectively) can be estimated using the Lorentz-Lorenz relation and the densities and compositions of the two phases,[8] or as is the case here, n_- and n_+ can be obtained from direct measurements. For the $CS_2 + CH_3OH$ mixture, for example, we find $n(\pm) = n_c + Bt \pm (\Delta n_0/2)t^\beta$, where $n_c = 1.5146$, $B = 0.053$, $\Delta_n = 0.394$, $t = (T_c - T)/T_c$, and $\beta = 0.325$. All three systems were analyzed in the same way and gave the same result when compared with theory. Values of n_c, B, and Δn_0 for the other two mixtures are included in Table I. For the refractive index and ellipticity measurements we used the HeNe wavelength $\lambda = 632.8$ nm.

The experimental values of $\bar{\rho}$ and η can be used to test various models of the refractive index profile. From a model of $n(z)$ one can compute $\bar{\rho}$ and compare the results

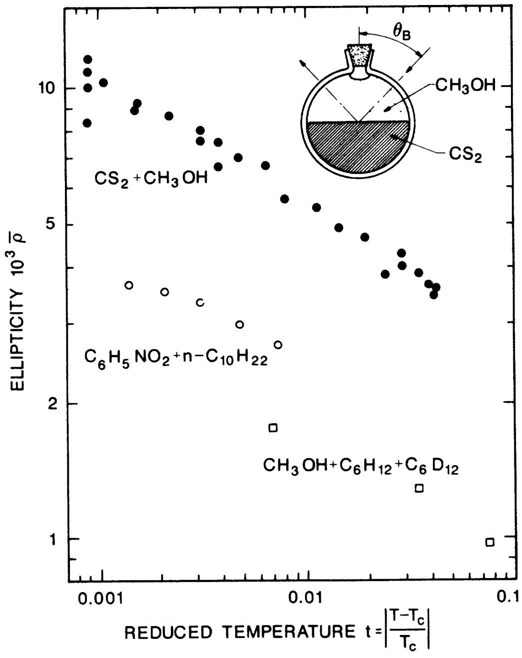

FIG. 1. Ellipticity $\bar{\rho}$ from the liquid-liquid interface of three mixtures. Solid circles: $CS_2 + CH_3OH$; open circles: $C_6H_5NO_2 + n\text{-}C_{10}H_{22}$; open squares: $CH_3OH + C_6H_{12} + C_6D_{12}$. The inset diagram shows the sample cell with light incident at Brewster's angle θ_B.

© 1988 The American Physical Society

TABLE I. Three mixtures compared.

Mixture	T_c (K)	n_c	B	Δn_0	σ_0 (erg/cm^2)	ξ_0^- (nm)	$\Delta\rho$ (q/cm^3)
CS_2+CH_3OH	309.30	1.5146	0.053	0.394	13.8	0.177	0.656
$CH_3OH+C_6H_{12}+C_6D_{12}$	319	1.378	0.0754	0.1365	16.8[a]	0.166[a]	0.0024
$C_6H_5NO_2+n\text{-}C_{10}H_{22}$	297.62	1.4659	0.0614	0.2216	31.0	0.117	0.7531

[a] Reference 10.

to the measured values. We will first take $n(z)$ from Fisk-Widom theory[3] and then look at the effects of capillary waves.

For Fisk-Widom theory we take $n(z)$ to be

$$n(z)=\tfrac{1}{2}(n_+ + n_-)+\tfrac{1}{2}(n_+ - n_-)X(z/2\delta)\,, \tag{2}$$

where the order-parameter profile $X(z/2\delta)$ is given by

$$X(z/2\delta)=\sqrt{2}\tanh(z/2\delta)[3-\tanh^2(z/2\delta)]^{-1/2}\,. \tag{3}$$

For a binary-liquid mixture, $X(z/2\delta)$ is related to the composition profile at a height z normal to the interface. In Fisk-Widom theory δ is equal to the bulk correlation length in either phase $\xi^- = \xi_0^- t^{-\nu}$, where $\nu = 0.625$. Once the amplitude ξ_0^- has been determined, $\bar{\rho}$ can be calculated without adjustable parameters.

We have determined ξ_0^- using a relation from two-scale-factor universality and a compilation of experimental data.[9,10] Specifically, $\sigma_0(\xi_0^-)^2/k_B T_c \simeq R$, where k_B is Boltzmann's constant, and σ_0 is the interfacial tension amplitude. At present there is a difference between the experimental value of the constant R ($=0.1047$) and the theoretical value ($R=0.128$). We have chosen the experimental value at this point but we will outline a method (put forward by Kayser[5] and extended by Van Leeuwen and Sengers[6]) to reconcile the two values later in this paper. For the CS_2+CH_3OH mixture, we have measured σ_0 to be 13.8 (mN/m) using the method of Chaar, Moldover, and Schmidt,[10] which implies that $\xi_0^- = 0.177$ nm. With this determination of ξ_0^-, the density profile theory of Fisk and Widom falls 20% below the experimental ellipticity. This is not surprising because we have not included the effects due to capillary waves. Even greater differences occurred for the two other systems $CH_3OH+C_6H_{12}+C_6D_{12}$ and $C_6H_5NO_2+n\text{-}C_{10}H_{22}$.

For a more realistic calculation capillary waves must be included. For the capillary-wave model we will use the self-consistent calculation of Van Leeuwen and Sengers[6] with the advantage that there are no adjustable parameters. Thus the number of capillary waves to be included is determined uniquely. Their approach extends the work of Kayser[5] in which he used one adjustable parameter (the short-wavelength cutoff l^*). l' (the vertical blob size) and l^* are determined by boundary conditions on the interfacial tension.

In capillary-wave theory, the capillary-wave mean-square amplitude is given by

$$\langle\zeta^2\rangle = \frac{k_B T_c}{(2\pi)^2}\int_0^{q_{\max}} \frac{d\bar{q}}{\sigma(q)q^2+2g\Delta\rho}\,, \tag{4}$$

where g is the acceleration due to gravity 980 cm/sec^2, $\Delta\rho$ is the density difference between the two phases $\Delta\rho_0 t^\beta$, and $\sigma(q)$ is the interfacial tension that is allowed to depend on the capillary-wave vector $\bar{q}$. The boundary conditions are $\sigma(q_{\max})=\sigma_b$(theory) and $\sigma(q=0)=\sigma$(expt) where $q_{\max}(=2\sqrt{\pi}/l^*)$ is the largest wave vector allowed by the theory. We have taken σ_b (theory) to be the Fisk-Widom value for the bare surface tension. The single degree of freedom present in Kayser's calculation is removed by demanding that the interfacial tension $\sigma(q)$ be maximum at $q=q_{\max}$, i.e., $[d\sigma(q)/dq]\,|_{q_{\max}}=0$, where

$$\sigma(q)=\sigma_b+\frac{k_B T_c}{8\pi^2(\xi^-)^2}\int_0^{2\pi} d\theta \int_q^{q_{\max}} q\,dq \ln\left(\frac{\sigma_b(l^* l')^2 q^2}{2\pi k_B T_c}\right)\,. \tag{5}$$

The above condition on the derivative of $\sigma(q)$ at $q_{\max}$ fixes the value of $l'=1.977\xi^-$. The value of l^* is then adjusted until $\sigma(q=0)=\sigma$(expt) with the result $l^*=4.74\xi^-$. $q_{\max}$ and $\sigma(q)$ are now completely determined and Eq. (4) can be integrated numerically to give the capillary-wave amplitude.

The capillary-wave contribution to the ellipticity $\bar{\rho}_{cw}$ at Brewster's angle for a sharp but rough interference is given by Beaglehole[11] and Zielinska, Bedeaux, and Vlieger[12] and depends linearly on $q_{\max}$.

$$\bar{\rho}_{cw}=\frac{3}{4}\left(\frac{\omega}{c}\right)\frac{n_+^2-n_-^2}{(n_+^2+n_-^2)^{1/2}}\frac{k_B T_c}{\sigma_b}\frac{q_{\max}}{2\pi}\,, \tag{6}$$

where $\omega/c=2\pi/\lambda$, σ_b is the bare surface tension and $q_{\max}$ is now equal to $2\sqrt{\pi}/4.74\xi^-$. The total ellipticity is given by the sum

$$\bar{\rho}_{tot}=\bar{\rho}_D+\bar{\rho}_{cw}\,. \tag{7}$$

Although the fit was moved in the right direction by the addition of capillary waves, the resulting $\bar{\rho}_{tot}$ is now too large. That the two contributions should be added directly rather than by adding the squares has been shown by Marvin and Toigo.[13]

A possible reason for this conflict between measured and calculated values of $\bar{\rho}$ may be due to an overlap of the two models since the Fisk-Widom theory includes a wide range of fluctuations but it is not known exactly which fluctuations have been included.[14] Another possible reason for the conflict may be that Eq. (6) has been developed only to first order in $\langle\zeta^2\rangle^{1/2}/\lambda$. Second-order terms, which have not been calculated, may be significant.[14] At present, however, the combined theory used here does give good agreement with sulfur hexafluoride (SF_6) when the reflectivity data of Wu and Webb[15] are used.

The quantity η in Eq. (1b) has been used to characterize the interface.[7,11] Recently, Beaglehole[16] measured η for pure carbon tetrachloride (CCl_4) near its critical point. In Fig. 2 we plot his data[16,17] for CCl_4 together with $|\eta|$ derived from our ellipticity data and Eq. (1a) for the mixture CS_2+CH_3OH. Our data for the pseudobinary system ($CH_3OH+C_6H_{12}+C_6D_{12}$) and the binary system ($C_6H_5NO_2+n\text{-}C_{10}H_{22}$) are also plotted at several temperatures. As can be seen from the data in Fig. 2 and from evaluating Eqs. (2) and (3) in Eq. (1b), the integral η is a system-dependent characteristic length that varies as the ellipsometric contrast $(n_+-n_-)^2$ for systems with comparable correlation lengths.

To compare results from different systems it is necessary to remove the dependence on the ellipsometric contrast and the correlation length. We, therefore, start by defining the universal quantity.

$$\chi_{\mathrm{mf}}=\int[1-X^2(y)]dy \quad =\text{universal constant}\simeq 2.28$$

which is an integral over the order-parameter profile $X(y)$ which is itself a universal function. χ_{mf} is related to the integral η through

$$|\eta|\simeq 2(n_+-n_-)^2\xi^-\chi_{\mathrm{mf}} \tag{8}$$

for temperatures in which the correlation length $\ll\lambda$ and where $|(n_-^2-n_+^2)/(n_+^2+n_-^2)|\ll 1$, which is the case for the fluids discussed in this work. Equation (7) can be rewritten using Eq. (1a) and Eqs. (6) and (8) as

$$\bar{\rho}_{\mathrm{tot}}=\frac{\pi}{\lambda}\frac{(n_+^2+n_-^2)^{1/2}}{n_+^2-n_-^2}2(n_+-n_-)^2\xi^-\chi_{\mathrm{mf}}+\frac{3\pi}{2\lambda}\frac{n_+^2-n_-^2}{(n_+^2+n_-^2)^{1/2}}\frac{\xi^-}{\tilde{\sigma}_b\sqrt{\pi}}\frac{1}{4.74} \tag{9a}$$

which simplifies to

$$\bar{\rho}_{\mathrm{tot}}\approx\frac{\sqrt{2}\pi}{\lambda}\xi^-\Delta n\left[x_{\mathrm{mf}}+\frac{3}{2\sqrt{\pi}}\left(\frac{1}{\tilde{\sigma}_b}\right)\frac{1}{4.74}\right] \tag{9b}$$

under the same conditions used to obtain Eq. (8). $\tilde{\sigma}_b$ is a dimensionless bare interfacial tension $\tilde{\sigma}_b\equiv\sigma_b(\xi^-)^2/k_BT_c=0.128$. If we define $\chi_{\mathrm{cw}}\equiv 3/2\sqrt{\pi}(1/\tilde{\sigma}_b 4.74)=1.39$ then Eq. (9b) can be written

$$\bar{\rho}_{\mathrm{tot}}\approx\frac{\sqrt{2}\pi}{\lambda}\xi^-\Delta n(\chi_{\mathrm{mf}}+\chi_{\mathrm{cw}}), \tag{10}$$

where $\chi=\chi_{\mathrm{mf}}+\chi_{\mathrm{cw}}$ is a universal constant. The values of χ obtained using the measured values of $\bar{\rho}$ and Eq. (10) are plotted in Fig. 3 for the three mixtures studied here. Note that within experimental uncertainty these three

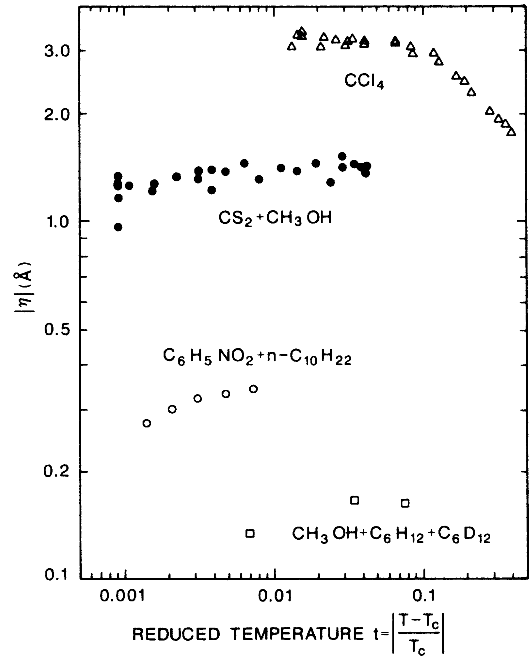

FIG. 2. The ellipsometric thickness $|\eta|$ is plotted vs temperature for three mixtures and one pure fluid. The symbols are the same as in Fig. 1. $|\eta|$ varies by an order of magnitude between mixtures depending on the optical contrast $(n_+-n_-)^2$. Additional open triangles represent CCl_4 data of Ref. 16.

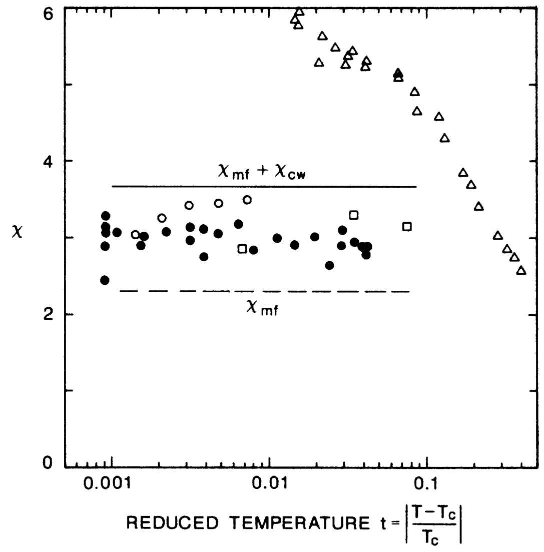

FIG. 3. When $|\eta|$ is scaled as indicated in the text, the fluid mixtures (CS_2+CH_3OH), ($CH_3OH+C_6H_{12}+C_6D_{12}$), and ($C_6H_5NO_2+n\text{-}C_{10}H_{22}$) give the same value for the universal constant χ. The theoretical value for χ ($=3.67$) is significantly higher. We were unable to scale the pure fluid CCl_4 (open triangles) to either the mixtures or the theoretical value of χ with the present model.

very different mixtures give the same value for χ. The calculated value of $\chi(=3.67)$, however, does not coincide with the measured values.

Figure 3 is thus our clearest indication of the disagreement between theory and experiment. The source of the disagreement is not known but it has been suggested[14] that the density profile theory may contain fluctuations that extend into the capillary-wave region. In effect this would cause an overcounting of modes and lead to the result displayed in Fig. 3. Calculations of the region of overlap have not yet appeared in the literature. Since the theory agrees with the reflectivity data of SF_6, an alternate explanation appears more likely. A second possible source for the disagreement is that Eq. (6) has been developed only to first order in $\langle\zeta^2\rangle^{1/2}/\lambda$. Second-order terms will tend to reduce the disagreement.[14]

The combined model as described above and the analysis summarized in Eq. (10) does not fit the CCl_4 data when values of n_-, n_+, σ, ξ^-, and $\Delta\rho$ appropriate to CCl_4 are used. As was done for the present mixtures, we have used the correlation length ξ^- in the two-phase region for the model. For CCl_4 Beaglehole obtains a good fit to the Fisk-Widom model in the small t region by identifying the characteristic length δ in Eqs. (2) and (3) with the correlation length on the critical isochore in the one-phase region $\xi^+(=1.95\xi^-)$. We see no reason to make such an identification. Further work is needed to resolve the differences between the liquid-mixture cases and the pure-fluid case. We have verified Beaglehole's datum for CCl_4 at $t=0.47$ using a photoelastically modulated ellipsometer based on his design.[11] We have not solved problems related to pressure-induced cell-window strain for pure fluids near their critical points and thus have not been able to confirm Beaglehole's higher pressure data where the model should apply. The liquid mixtures we used have an advantage for the experimenter in that their vapor pressures near the consolute temperatures are less than 1 atm; thus, pressure-dependent cell-window strain does not interfere with the ellipticity measurements. Other precautions that we have taken include four-stage thermostatting with mK temperature control, thorough *in situ* stirring, and *in situ* refractive index measurements.[18] The ellipticity measurements for CS_2+CH_3OH were repeated in two separate fused silica cells and gave the same result.

I would like to thank R. F. Kayser, M. R. Moldover, and J. Sengers for many helpful discussions on this subject. I would also like to thank D. Jasnow and M. Schneider for their help. This work has been supported in part by NASA under Contract No. H-27954-B.

---

[1] J. D. van der Waals, Z. Phys. Chem. **13**, 657 (1894).
[2] J. W. Cahn and J. E. Hilliard, J. Chem. Phys. **28**, 258 (1958).
[3] S. Fisk and B. Widom, J. Chem. Phys. **50**, 3219 (1969); J. S. Rowlinson and B. Widom, *Molecular Theory of Capillarity* (Oxford Univ. Press, London, 1982).
[4] F. P. Buff, R. A. Lovett, and F. H. Stillinger, Phys. Rev. Lett. **15**, 621 (1965).
[5] R. F. Kayser, Phys. Rev. A **33**, 1948 (1986).
[6] J. M. J. Van Leeuwen and J. V. Sengers (unpublished).
[7] P. W. Drude, *Theory of Optics* (Longmans, Green, and Co., New York, 1902).
[8] E. C. McKelvy and D. H. Simpson, J. Am. Chem. Soc. **44**, 105 (1922).
[9] M. R. Moldover, Phys. Rev. A **31**, 1022 (1985).
[10] H. Chaar, M. R. Moldover, and J. W. Schmidt, J. Chem. Phys. **85**, 418 (1986).
[11] D. Beaglehole, Physica B **100**, 163 (1980).
[12] B. J. A. Zielinska, D. Bedeaux, and J. Vlieger, Physica A **107**, 91 (1981).
[13] A. M. Marvin and F. Toigo, Phys. Rev. A **26**, 2927 (1982).
[14] R. F. Kayser and D. Bedeaux (private communications).
[15] E. S. Wu and W. W. Webb, Phys. Rev. A **8**, 2077 (1973).
[16] D. Beaglehole, Phys. Rev. Lett. **58**, 1434 (1987).
[17] D. Beaglehole, Physica B **112**, 320 (1982). The ellipticity of the mixture cyclohexane+aniline was measured in this work. We have not included this mixture in the present analysis because the measured surface tension for this mixture does not follow critical behavior for $t > 0.003$.
[18] J. W. Schmidt and M. R. Moldover, J. Chem. Phys. **84**, 4563 (1986).

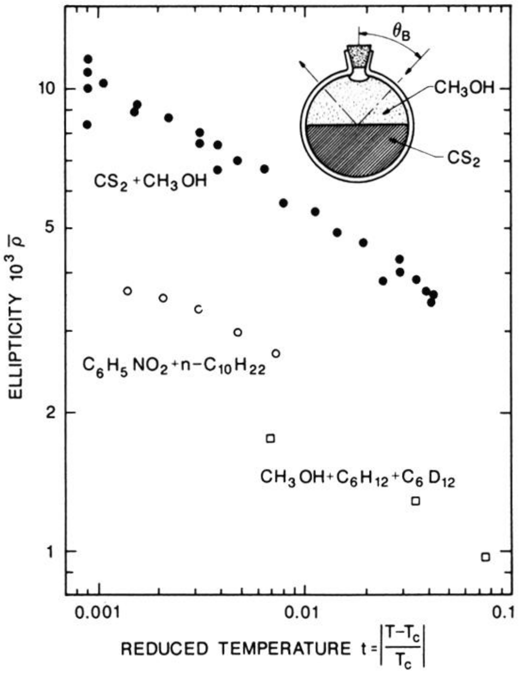

FIG. 1. Ellipticity $\bar{\rho}$ from the liquid-liquid interface of three mixtures. Solid circles: $CS_2 + CH_3OH$; open circles: $C_6H_5NO_2 + n\text{-}C_{10}H_{22}$; open squares: $CH_3OH + C_6H_{12} + C_6D_{12}$. The inset diagram shows the sample cell with light incident at Brewster's angle θ_B.